

All optical chaos synchronization between nonidentical optomechanical cavities

Souvik Mondal,¹ Murilo S. Baptista,² and Kapil Debnath^{2,*}

¹*Electronics and Electrical Communication Engineering Department, IIT Kharagpur, West Bengal, 721302, India*

²*School of Natural and Computing Sciences, University of Aberdeen, Aberdeen AB24 3UE, United Kingdom*

Optomechanical cavities, with nonlinear photon-phonon interactions, offer a more compact approach to chaos generation than conventional feedback-based optical systems. However, proper study on long-distance chaos synchronization of two optomechanical cavities connected by a long optical fiber is still unexplored. In this work, we theoretically investigate all-optical complete synchronization between unidirectionally coupled optomechanical cavities. Traditionally, achieving complete synchronization in nonlinear coupled oscillators and in optical systems necessitates identical systems. Our findings, which arise naturally from the fundamental mathematical properties of optomechanical cavities, demonstrate that parameter heterogeneity can, in fact, not only enable complete synchronization but make it stable.

The study of nonlinear dynamics and chaos has significantly advanced science and technology, offering fresh insights across various fields such as biology, chemistry, physics and many others [1, 2]. These advances have facilitated better understanding of complex dynamics that exhibits unpredictable behaviours [3]. From a technological standpoint, a pivotal moment in this scientific journey occurred in 1990, when Pecora and Carroll demonstrated that even chaotic systems possessing sensibility to the initial conditions and generating unpredictable behaviour could achieve complete synchronization, a concept traditionally associated with order [4]. The discovery of chaos synchronization has since become a cornerstone for innovative applications in secure communications [5], cryptography [6], distributed sensor networks [7] and artificial neural networks [8].

Among various platforms, optical systems, with their inherent advantages – such as wide bandwidth, higher dimensionality, and seamless integration with existing fibre optic networks [9] – are increasingly recognized as the ideal platform for demonstrating chaos synchronization and its applications. Optical systems designed with a master (transmitter) coupled unidirectionally to a slave (receiver) are particularly advantageous for securely transmitting information over long distances with high transmission rates and high bandwidth [10–15]. The optical system consists of a semiconductor laser with delayed feedback where the feedback is realized by purely optical or electro-optical nature [16]. This configuration often leads to bulky and complex setups. Optomechanical cavities (OMCs), by leveraging the inherent nonlinear interaction between light fields and mechanical oscillations, provide a fundamentally different approach to chaos generation which does not require any feedback loops [17–20]. While progress has been made in the study and generation of chaos in OMCs [21–24], the field still lacks comprehensive studies on long-distance chaos synchronization. To date, chaos synchronization has been observed between pump and probe fields in an OMC

mediated through mechanical vibrations [25, 26], which did not consider the spatially separated OMC configuration. This provides motivation to theoretically examine the use of OMCs in demonstrating all-optical long-distance chaos synchronization between two OMCs connected by a long optical fiber.

The synchronization of chaotic dynamics occurs in several forms [27–29] and, among them, our particular interest lies in studying complete chaos synchronization in OMCs, as it is the “strongest” form of synchronization where the state of the systems are exactly the same [28]. In the conventional optical system as well as in general coupled nonlinear oscillators, such a form of synchronization requires the system parameters to be identical or nearly identical [30–33], which poses a challenging task in practical implementation. Chaos synchronization in non-identical oscillators can induce weaker forms of synchronization, such as generalized synchronization [34], cluster synchronization [35–37] or phase synchronization [38, 39]. Recently, Sugitani *et al.* [40] showed that random heterogeneity facilitate global chaos synchronization in the regime of lower coupling strength. These recent works however deal with synchronization of nonidentical oscillators in a large complex network, not in the master slave configuration ideal for communication applications. So, apart from exploring the possibility of all optical long distance synchronization in OMCs, we also investigated how large parameter heterogeneity induces complete and stable synchronization of optical chaos. To demonstrate this idea we considered a simple configuration of master and slave OMC coupled by a long optical fiber in an unidirectional manner, and there is an additional presence of a phase controller element at the input of the slave cavity.

Our system, as shown in Fig. 1, consists of two microtoroid based OMCs [41–43] which are unidirectionally coupled from cavity 1 (master) to cavity 2 (slave) by an optical fiber with η being the efficiency of the fiber. We assume that each of the cavities has a dimensionless and complex optical mode amplitude $a_{1,2}$ and mechanical mode amplitude $b_{1,2}$, where the subindex “1” represents master, and “2” represents the slave. The intrinsic loss

* kapil.debnath@abdn.ac.uk

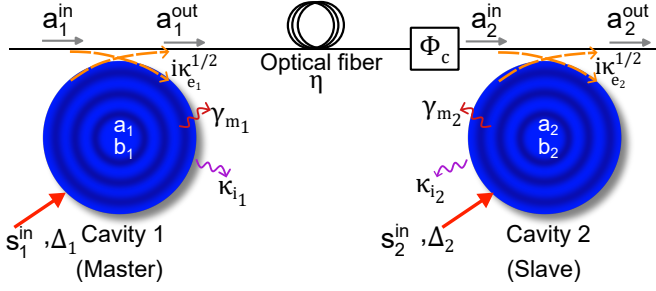


FIG. 1. Schematic of a master and a slave OMC coupled unidirectionally by optical fiber with the excitation laser being provided separately with amplitude $s_{1,2}^{\text{in}}$ and detuning $\Delta_{1,2}$. The phase controller block “ Φ_c ” adjusts the phase of the optical field coming from master cavity to realize chaos synchronization.

rate of the optical mode in the cavities is given by $\kappa_{i,2}$ while $\gamma_{m,2}$ is the loss rate corresponding to mechanical mode. The external coupling rate between the cavity and the waveguide (or fiber) is given by $\kappa_{e,2}$. We consider the cavities to be excited by lasers with amplitude $s_{1,2}^{\text{in}}$ and detuning $\Delta_{1,2}$ through the waveguide-cavity coupling mechanism with external coupling rate $\kappa_{s,2}$ (not shown explicitly in Fig. 1). The input (output) optical field of the cavities is labeled by $a_{1,2}^{\text{in}}$ ($a_{1,2}^{\text{out}}$). The detuning is given by the difference between laser frequency (ω_L) and the optical resonance frequency ($\omega_{c,2}$), which is, $\Delta_{1,2} = \omega_L - \omega_{c,2}$. The block labeled by “ Φ_c ” is the phase controller block which adjusts the phase of the propagation delayed optical field a_{out}^1 and the resultant field is fed into cavity 2. This block serves an important role in synchronization as discussed later and such block can be experimentally realized by using an optical delay line circuits [44, 45]. The efficiency η of the optical fiber is set to 1, as we assume that amplifiers can be placed along the way. The equation of motions of the variables $a_{1,2}$ and $b_{1,2}$, for a noiseless configuration, are written as

$$\frac{da_{1,2}}{dt} = i \left(\Delta_{1,2} - \frac{\kappa_{1,2}}{2} \right) a_{1,2} - i2g_{0,2} \text{Re}(b_{1,2}) a_{1,2} + i\sqrt{\kappa_{s,2}} s_{1,2}^{\text{in}} + i\sqrt{\kappa_{e,2}} a_{1,2}^{\text{in}}, \quad (1a)$$

$$\frac{db_{1,2}}{dt} = - \left(i\omega_{m,2} + \frac{\gamma_{m,2}}{2} \right) b_{1,2} - ig_{0,2} |a_{1,2}|^2, \quad (1b)$$

where $g_{0,2}$ is the optomechanical coupling rate and $\omega_{m,2}$ is the resonance frequency of the mechanical modes in both the cavities. The total loss rate of the optical mode in each of the cavity is given by $\kappa_{1(2)} = \kappa_{i(2)} + \kappa_{s(2)} + \kappa_{e(2)}$. The last two terms of Eq. (1a) are the driving terms from the laser source with amplitude $s_{1,2}^{\text{in}}$ and the optical field $a_{1,2}^{\text{in}}$ respectively. The phase $+i$ of the coupling term $\sqrt{\kappa_{e,2}}$ and $\sqrt{\kappa_{s,2}}$ in the dynamical equation is arbitrarily chosen based on the choice of reference plane [46]. We assume no noise is added by the fiber, a realistic modeling assumption when the

master-slave synchronization is sufficiently stable to filter out noise in the receiver in an environment with a sufficiently large Signal to Noise Ratio. In this scenario, we set input field to cavity 1 $a_1^{\text{in}} = 0$ and the output field reduced to $a_1^{\text{out}} = a_1^{\text{in}} + i\sqrt{\kappa_{e1}} a_1 = i\sqrt{\kappa_{e1}} a_1$. On the other hand, the input field a_2^{in} of cavity 2 is the optical field coming from output field a_1^{out} of cavity 1 that experiences propagation delay in the long-distance fiber as well as adjustment of phase in the phase controller block. Therefore, $a_2^{\text{in}} = a_1^{\text{out}} e^{i(\phi_d + \phi_c)}$, where ϕ_d and ϕ_c are the propagation delay phase and the controlling phase respectively. Now, for convenience, we assume that the mechanical resonance frequencies and optomechanical coupling rates are similar, that is, $\omega_{m1} = \omega_{m2} = \omega_m$ and $g_{01} = g_{02} = g_0$. For further numerical computation, we work with re-scaled dynamical variables $\alpha_{1,2} = [\omega_m / (2\sqrt{\kappa_{s,2}} s_{1,2}^{\text{in}})] a_{1,2}$, $\beta_{1,2} = (g_0/\omega_m) b_{1,2}$ and the normalized parameters with respect to ω_m . Therefore, the equations of the motion are written as [19, 47]

$$\frac{d\alpha_1}{d\tau} = \left(i \frac{\Delta_1}{\omega_m} - \frac{\kappa_1}{2\omega_m} \right) \alpha_1 - i2g_0 \text{Re}(\beta_1) \alpha_1 + i \frac{1}{2}, \quad (2a)$$

$$\frac{d\alpha_2}{d\tau} = \left(i \frac{\Delta_2}{\omega_m} - \frac{\kappa_2}{2\omega_m} \right) \alpha_2 - i2g_0 \text{Re}(\beta_2) \alpha_2 - \frac{\sqrt{\kappa_{e1}} \kappa_{e2} \sqrt{\kappa_{s1}} s_1^{\text{in}}}{\omega_m \sqrt{\kappa_{s2}} s_2^{\text{in}}} e^{i(\phi_c + \phi_d)} \alpha_1 + i \frac{1}{2}, \quad (2b)$$

$$\frac{d\beta_{1,2}}{d\tau} = - \left(i + \frac{\gamma_{m,2}}{2\omega_m} \right) \beta_{1,2} - i \frac{P_{1,2}}{2} |\alpha_{1,2}|^2, \quad (2c)$$

where the dimensionless time is given by $\tau = \omega_m t$ and the dimensionless power $P_{1,2} = 8\kappa_{s,2} (s_{1,2}^{\text{in}})^2 g_0^2 / \omega_m^4$.

Complete chaos synchronization between the coupled optomechanical cavities is achievable when the mathematical form of the dynamical equations of the cavities in Eq. (2) become identical. Now, we assume that the solution of Eq. (2) lies on the synchronization manifold, that is $\vec{x}_1(\tau) = \vec{x}_2(\tau) \equiv \vec{s}(\tau)$ in which $\vec{x}_1 = (\alpha_1, \beta_1)$, $\vec{x}_2 = (\alpha_2, \beta_2)$ and $\vec{s} = (\alpha, \beta)$; and substituted them in Eqs. (2). Thereby, we obtain the necessary conditions for complete synchronization (i.e., the existence of the synchronization manifold) in which the decay rates needs to be identical, which is,

$$\kappa_1 = \kappa_2 \quad \text{and} \quad \gamma_{m1} = \gamma_{m2}, \quad (3)$$

dimensionless power needs to equivalent, that is,

$$P_1 = P_2 \quad \text{or} \quad \sqrt{\kappa_{s1}} s_1^{\text{in}} = \sqrt{\kappa_{s2}} s_2^{\text{in}}, \quad (4)$$

and lastly with the use of the condition in Eq. (4) the detuning of the two cavities satisfy

$$\Delta_1 - \Delta_2 = \sqrt{\kappa_{e1} \kappa_{e2}} \frac{\sqrt{\kappa_{s1}} s_1^{\text{in}}}{\sqrt{\kappa_{s2}} s_2^{\text{in}}} = \sqrt{\kappa_{e1} \kappa_{e2}}, \quad (5)$$

provided the coupling phase factor in Eq. (2b) is maintained at

$$e^{i(\phi_d + \phi_c)} = -i. \quad (6)$$

The choice of imaginary coupling phase factor in Eq. (6) ensures that the optical field from cavity 1 modifies the detuning of cavity 2. By fixing Δ_1 and Δ_2 at optimum values satisfying Eq. (5), the effective detuning in cavity 2 (given by $\Delta_2^{\text{eff}} = \Delta_2 + \sqrt{\kappa_{e_1}\kappa_{e_2}}$) matches that of detuning in cavity 1 at the synchronization manifold. Effectively, the cavities possess identical detuning values and if the other mentioned parameters are equal, similar dynamical response is expected in the cavities and thus complete chaos synchronization is an allowed solution of Eqs. (2). Since $\kappa_{e_{1,2}} \neq 0$, the actual detuning in the cavities has to be different, which is $\Delta_1 \neq \Delta_2$, and thereby follows a counter-intuitive approach as in general cases all the possible parameters in coupled optical nonlinear oscillators are equivalent. There can be also alternative situation for complete synchronization, where $e^{i(\phi_d + \phi_c)} = i$ leading to the condition $\Delta_2 - \Delta_1 = \sqrt{\kappa_{e_1}\kappa_{e_2}}$, but it induce poor synchronization which is further discussed later. The adjustment of the detuning values is feasible experimentally by changing the optical resonance frequency in each of the cavity [48–50]. The propagation delay phase ϕ_d is determined by the length of the optical fiber, while the ϕ_c is adjusted by the phase controller block, and therefore, the combination of these decides the overall coupling phase factor.

In addition, the quality of chaos synchronization is quantified in terms of the correlation coefficient involving optical intracavity intensity dynamics $I_{1,2} = |\alpha_{1,2}|^2$,

$$C = \frac{\langle [I_1(\tau) - \langle I_1(\tau) \rangle] [I_2(\tau) - \langle I_2(\tau) \rangle] \rangle}{\sqrt{\langle [I_1(\tau) - \langle I_1(\tau) \rangle]^2 \rangle \langle [I_2(\tau) - \langle I_2(\tau) \rangle]^2 \rangle}}, \quad (7)$$

where $\langle \cdot \rangle$ is the time average of intracavity intensity dynamics. The stability of the complete synchronization manifold is addressed by calculating the maximum of transverse Lyapunov exponent ($\lambda_{\perp}^{\text{max}}$) obtained from the variational equation of error dynamics [51]. For stability, $\lambda_{\perp}^{\text{max}}$ must have negative value, indicating that any deviation from the synchronization manifold will eventually revert back to the manifold. The error between the cavities is given by $\vec{e}(\tau) = \vec{x}_1(\tau) - \vec{x}_2(\tau)$ and the vectors \vec{x}_1, \vec{x}_2 are reassigned to real elements by expressing $\alpha_{1,2} = \alpha_{r,1,2} + i\alpha_{i,1,2}$ and $\beta_{1,2} = \beta_{r,1,2} + i\beta_{i,1,2}$. The vectors of small quantities are then written as $\delta\vec{x}_{1,2} = (\delta\alpha_{r,1,2}, \delta\alpha_{i,1,2}, \delta\beta_{r,1,2}, \delta\beta_{i,1,2})$ and therefore $\delta\vec{e} = \delta\vec{x}_1 - \delta\vec{x}_2$. The linearized equation of the error dynamics $\delta\vec{e}_{1,2}$ is written as

$$\frac{d\delta\vec{e}}{d\tau} = M\delta\vec{e}, \quad (8)$$

where M is the Jacobian matrix calculated at the synchronization manifold $\vec{s} = (\alpha_r, \alpha_i, \beta_r, \beta_i)$ given by

$$M = \begin{pmatrix} -\frac{\kappa}{2\omega_m} & -\frac{\Delta_2^{\text{sync}}}{\omega_m} + 2\beta_r & 2\alpha_i & 0 \\ \frac{\Delta_2^{\text{sync}}}{\omega_m} + 2\beta_r & -\frac{\kappa}{2\omega_m} & -2\alpha_r & 0 \\ 0 & 0 & -\frac{\gamma_m}{2\omega_m} & 1 \\ -P\alpha_r & -P\alpha_i & -1 & -\frac{\gamma_m}{2\omega_m} \end{pmatrix}, \quad (9)$$

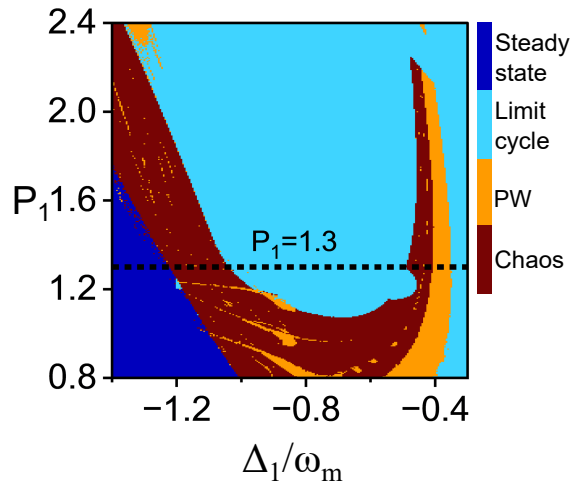


FIG. 2. The parameter space of P_1 and Δ_1 of cavity 1 illustrating regions of steady state, limit cycle, periodic windows (PWs) and chaos. The same is valid for cavity 2 as well, if uncoupled. The horizontal dashed line at $P_1 = 1.3$ is the operating dimensionless power level of both cavity 1 and cavity 2.

and Δ_2^{sync} satisfies Eq. (5).

Prior to delving into the discussion on synchronization, we first analyzed various nonlinear regimes in the OMC for the uncoupled case, focusing in the parameter space of dimensionless power (P_1 or P_2) and detuning (Δ_1 or Δ_2). Equations (2) are numerically solved for $\kappa_{e_{1,2}} = 0$ by using Runge-Kutta method with the parameters κ_1 and γ_{m_1} fixed at $0.73\omega_m$ and $7.7 \times 10^{-3}\omega_m$ respectively [26], while P_1 and Δ_1 are varied for the master cavity. We identified steady state region that dominates in the large values of detuning and observed nonlinear regimes namely limit cycle (i.e., for this work we assume it to be a period-one orbit), periodic windows, PWs, (regions of parameter space presenting a cascade of limit cycles that can lead or bifurcate via period doubling into chaos by a parameter alteration) and chaos, as shown in Fig. 2. The chaotic regimes are confirmed by the positive maximal Lyapunov exponent λ_{max} which gives the rate of divergence of two infinitesimally close trajectories in the phase space [3, 52]. The chaotic regime at lower P_1 values in Fig. 2 spreads across wide range of Δ_1 , in which certain regions are occupied by the PWs. However from about $P_1 \approx 1$, the chaotic regime starts to divide into two arms; one in the low detuned values, while other in the high detuned values. As P_1 increases, the chaotic regime in the left arm starts to diverge further from the right arm, with limit cycles occupying the region between them and the regime in the left arm gradually reduces to non-chaotic state.

Figure 3(a) shows a typical bifurcation diagram of the master cavity as a function of Δ_1 at fixed $P_1 = 1.3$ when the cavities are uncoupled, highlighting different dynamical regimes of mechanical oscillations. The positive values of the λ_{max} in Fig. 3(b) implies chaotic oscillations.

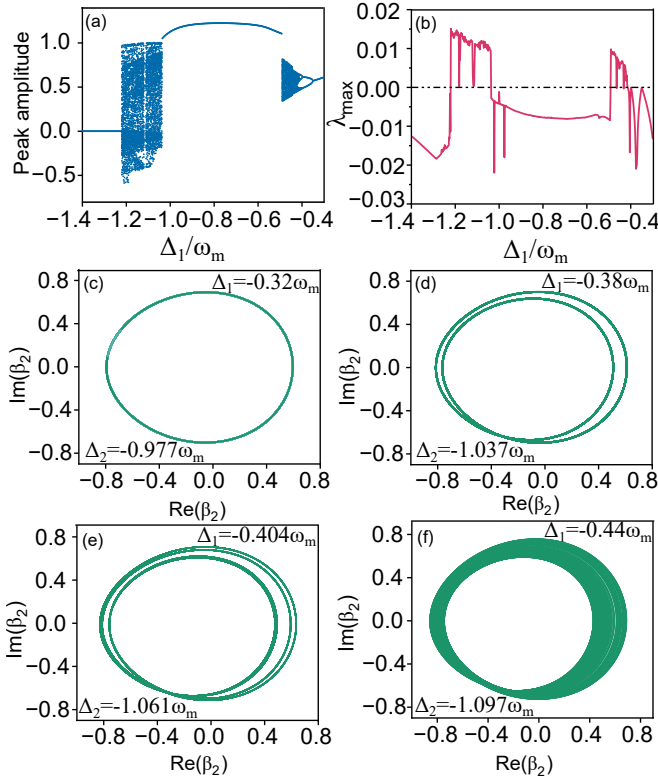


FIG. 3. (a) The bifurcation diagram of the master cavity obtained by collecting peaks of mechanical oscillations under varying Δ_1 for uncoupled configuration. (b) The maximal Lyapunov exponent λ_{\max} of the bifurcation plot. (c)-(f) The mechanical phase space plots of the slave cavity in the coupled configuration showing period-1, period-2, period-4 orbit and chaos respectively in which the value of Δ_2 's are obtained from synchronization criteria in Eq. (5). All the plots are obtained for $P = 1.3$ and $\kappa_e = 0.9\kappa$ with the initial values of all the dynamical variables set to zero.

Now, we study the mechanical response of the system for coupled configuration i.e., $\kappa_{e1,2} \neq 0$. In the numerical simulations, the cavities are operated at same power level satisfying Eq. (4), which is $P_1 = P_2 = P = 1.3$. The decay rates are also kept identical satisfying Eq. (3), that is, $\kappa_1 = \kappa_2 = \kappa = 0.73\omega_m$, $\gamma_{m1} = \gamma_{m2} = \gamma_m = 7.7 \times 10^{-3}\omega_m$. For convenience, we considered external coupling rate to be equal, which is, $\kappa_{e1} = \kappa_{e2} = \kappa_e$ and of the high magnitude of $\kappa_e = 0.9\kappa$. We also maintained the condition in Eq. (6). To demonstrate synchronization, we start with observing the mechanical response of the slave cavity by changing the dynamical state of the master cavity from non-chaotic to chaotic state by varying Δ_1 . The detunings of the master cavity are set to $\Delta_1 = (-0.32\omega_m, -0.38\omega_m, -0.404\omega_m, -0.44\omega_m)$, as indicated by the vertical dashed line in Fig. 3(a) which corresponds to period-1, period-2, period-4 orbit, and chaos, respectively. By tuning Δ_2 of the slave cavity according to Eq. (5) to values $\Delta_2 = (-0.977\omega_m, -1.037\omega_m, -1.061\omega_m, -1.097\omega_m)$, the cavity precisely follows the same path to chaos and similar

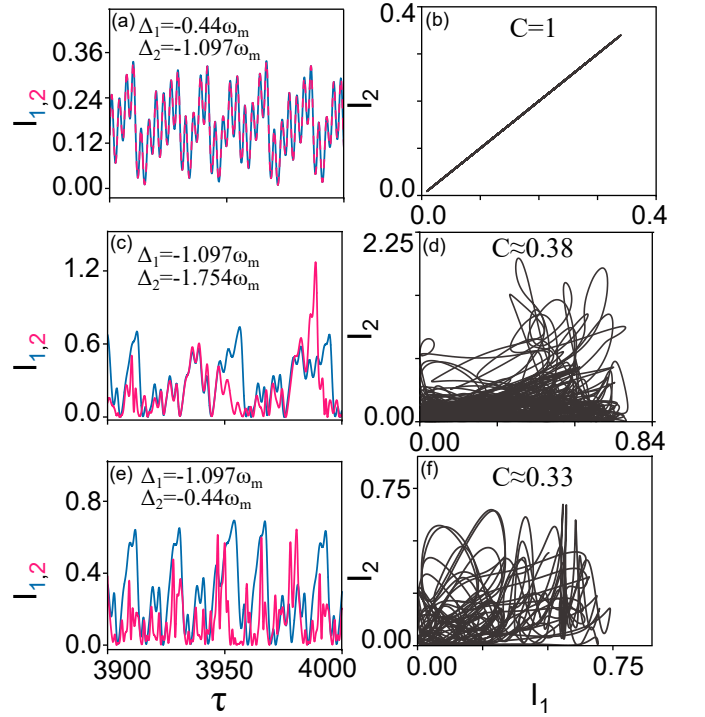


FIG. 4. (a) The synchronized intracavity intensity dynamics at $\Delta_1 = -0.44\omega_m$, $\Delta_2 = \Delta_1 - \kappa_e = -1.097\omega_m$ and (b) the projection of chaotic attractor in I_1 - I_2 plane with $C = 1$. (c) The intracavity intensity dynamics at $\Delta_1 = -1.097\omega_m$, $\Delta_2 = \Delta_1 - \kappa_e = -1.754\omega_m$ and (d) the chaotic attractor in the I_1 - I_2 plane with $C \approx 0.38$. (e) The intracavity intensity dynamics at $\Delta_1 = -1.097\omega_m$, $\Delta_2 = \Delta_1 + \kappa_e = -0.44\omega_m$ and (f) its corresponding chaotic attractor in the I_1 - I_2 plane with poor $C \approx 0.33$.

mechanical response as the master cavity, as illustrated in the mechanical phase space plots in Fig. 3(c)-(f). The range of values for Δ_2 differs from that of Δ_1 , which would lead to a vastly different response in the slave cavity if it were uncoupled. In our coupled configuration, with heterogeneity in the detuning values, the slave cavity is completely synchronous to master cavity for each attractor within parameters leading to chaos via periodic doubling route.

We further explain the occurrence of synchronized chaos in Fig. 3(f) through the corresponding temporal dynamics of intracavity intensity, $I_{1,2}$. Similar to the mechanical dynamics, intracavity intensity in the slave becomes completely synchronous to the trajectories of master cavity as shown in Fig. 4(a). To confirm complete synchronization, the projection of the chaotic attractor of the coupled configuration in the plane of I_1 - I_2 lies in the identical line as shown in Fig. 4(b). By using Eq. (8) and (9), the transverse Lyapunov spectrum is obtained to get $\lambda_{\perp}^{\max} \approx -0.006$, which imply that this synchronization manifold is linearly stable. A physical explanation for the emergence of complete synchronization can be cast in terms of distribution of energies in the coupled cavities. Since, the master cavity is excited

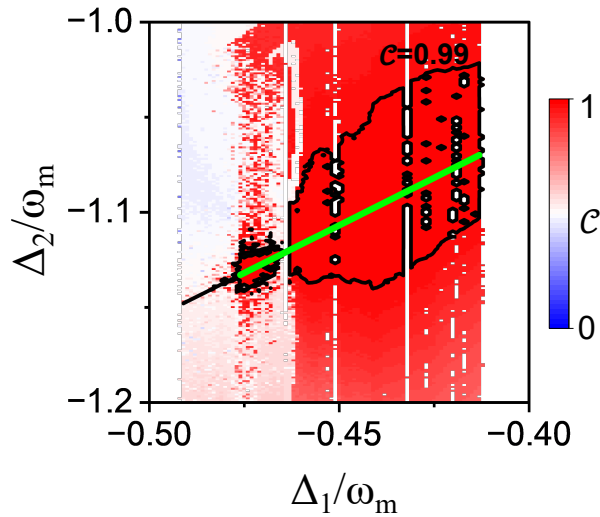


FIG. 5. The quality of chaos synchronization for varying Δ_1 and Δ_2 at fixed $P = 1.3$ and $\kappa_e = 0.9\kappa$. The white regions denote parameters that lead the master cavity to present periodic attractors.

with laser of low detuning compared to the slave, more photons are injected into the master cavity. But the unidirectional coupling results in the flow of optical energy from master to slave making the distribution of energy similar in both the cavities. Equivalently, this flow of energy results in modifications of effective detuning of the slave which give rise to identical dynamical responses. Since external coupling rate $\kappa_{e1,2}$ is responsible for the amount of flow, tuning them to the sufficiently strong and optimum value leads to synchronization.

Now, for same $P = 1.3$ and $\kappa_e = 0.9\kappa$, detuning of the master cavity is kept in the higher value at $\Delta_1 = -1.097\omega_m$, while the slave at $\Delta_2 = -1.754\omega_m$ satisfying Eq. (5) and maintaining Eq. (6) in the simulation. The intracavity dynamics in Fig. 4(c) suggests that the chaotic dynamics of the cavities are unable to synchronize perfectly despite the existence of synchronization manifold and also the projection of the chaotic attractor in the I_1 - I_2 plane in Fig. 4(d) is very complicated with poor correlation value $\mathcal{C} \approx 0.38$. Here, the slave cavity experiences optical field from the master cavity which has stronger modulations in its chaotic waveform waveform and higher Lyapunov exponent (see Fig. 3(a) and 3(b)). This makes the trajectory path in the phase space more complex and diverge at a faster rate, and the current value of κ_e is not sufficiently strong to support synchronization of such complicated chaotic waveform. Next, the numerical simulations are adjusted to satisfy the alternate criteria, where $\Delta_2 - \Delta_1 = \sqrt{\kappa_{e1}\kappa_{e2}}$ for $e^{i(\phi_a + \phi_c)} = i$. The dynamics plotted in Fig. 4(e) for $\Delta_1 = -1.097\omega_m$ and $\Delta_2 = -0.44\omega_m$, still not able to synchronize completely. Chaos synchronization is very poor with $\mathcal{C} \approx 0.33$ and is evident with the nature of the chaotic attractor in the plane of I_1 and I_2 in Fig. 4(f). This occurs since energy distributions become asymmet-

rical as Δ_1 is higher than Δ_2 . Additionally, the master cavity produces more modulated chaotic waveform at this value of Δ_2 and with the current magnitude of κ_e , the synchronization becomes poor.

To have an idea of possible operating values of complete synchronization, we plot a correlation map for varying Δ_1 and Δ_2 in Fig. 5 by keeping P and κ_e same as before. The green line indicates parameters for which complete synchronization of chaotic trajectories in master and in the slave is stable. The quality of chaos synchronization is high around this line as evident from the black contour of $\mathcal{C} = 0.99$, but decreases as we go away from it. Further details on the threshold external coupling rate and dimensionless power for synchronization are provided in the Appendix.

In summary, we have demonstrated stable, complete chaos synchronization in a master-slave configuration of two optomechanical cavities coupled unidirectionally over long distances. By deriving synchronization criteria that highlight the critical role of detuning heterogeneity in the order of the total cavity decay rate, we have identified a broad and accessible parameter space for achieving stable synchronization. This work represents the first demonstration of long-distance chaos synchronization in an optomechanical system, offering a fully all-optical, compact, and efficient solution. We believe that our findings will open new avenues for innovative approaches in secure chaos-based communication by leveraging synchronized master-slave configurations, which inherently filter noise and provide robust performance even in noisy communication channels. Popular approaches such as the chaos-shift-keying method [53] based on a master-slave configuration that sends a bit by making parameters of the master to mismatch the ones in the receiver are vulnerable to noise, as parameter mismatches make synchronization unstable, and noise cannot be properly filtered out. However, for the proposed systems of OMCs, parameters can be changed, inducing a change in the attractors and that can be sensed in the receiver ending (slave), still preserving the stability of the synchronization manifold, thus, allowing transmission of information by a parameter shift that is still robust to noise in the channel. Moreover, if this parameter change is made following a communication protocol that is only known to transmitter (master) and receiver (slave), the transient nature of the trajectories might increase further the masking character of master-slave communication, potentially allowing for a de facto secure physical level chaos-based communication. By bridging fundamental advances in chaos synchronization with practical applications, this study establishes a scalable framework for secure, high-speed optical communication, contributing to both the fundamental understanding and technological utility of optomechanical systems.

We would like to express our gratitude to Prof. Celso Grebogi for insightful discussions. Souvik Mondal acknowledges support from Ministry of Education-STARs project, MoE-STARs/STARs-2/2023-0486. For the pur-

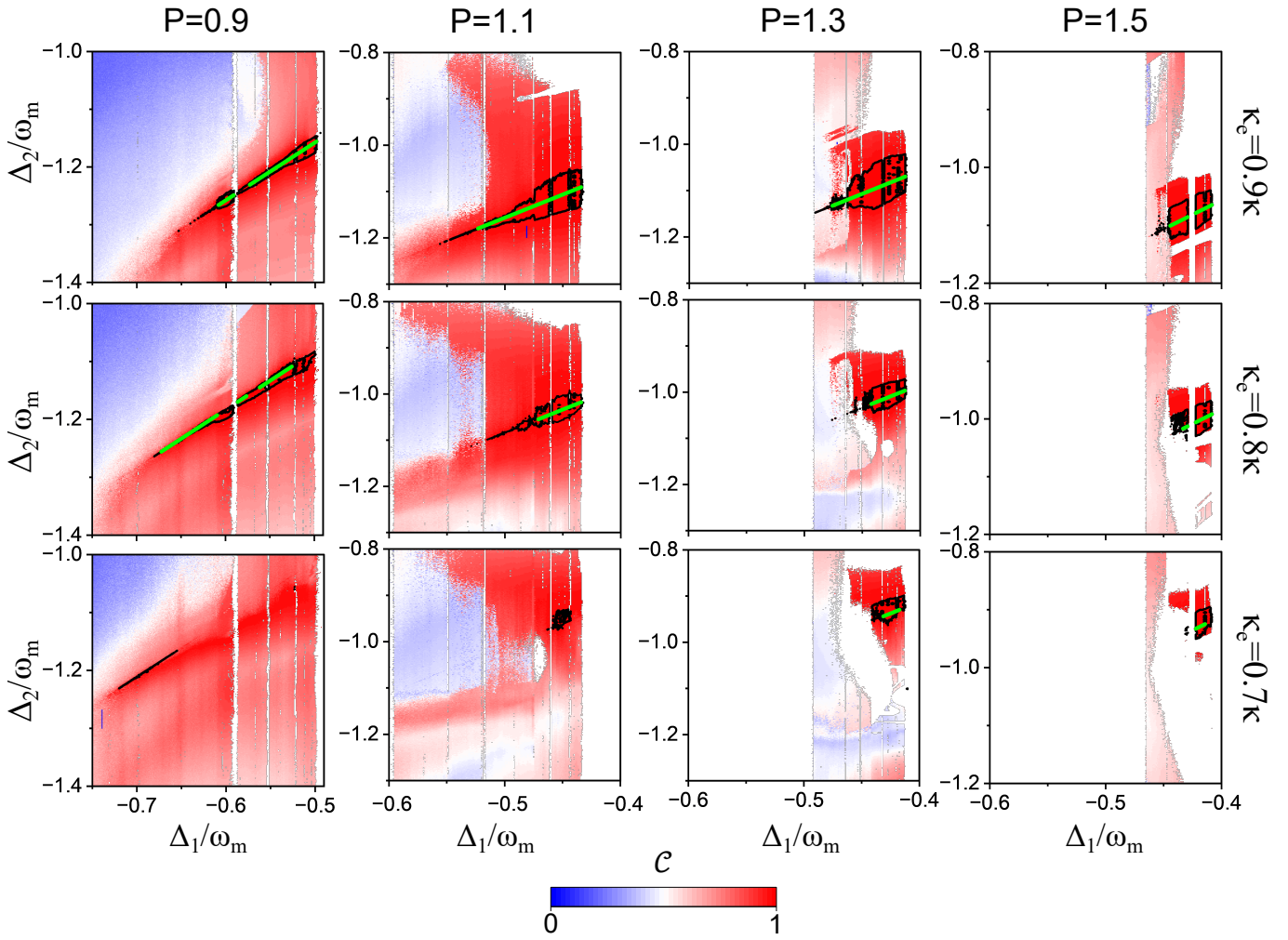


FIG. 6. A detailed parameter space of the chaos synchronization quantified with correlation coefficient C in the space of (Δ_1, Δ_2) for external coupling rate $\kappa_e = (0.7\kappa, 0.8\kappa, 0.9\kappa)$ and this is evaluated for $P = 0.9, P = 1.1, P = 1.3$ and $P = 1.5$.

pose of open access, the author has applied a Creative Commons Attribution (CC BY) license to any Author Accepted Manuscript version arising from this submission.

Appendix A: Dependence of chaos quality on dimensionless power and external coupling rate

In this section we discuss in detail how the chaos synchronization behaves for different values of P and κ_e . A two dimensional map, in the parameter space of (Δ_1, Δ_2) is plotted in Fig. 6 depicting the quality of chaos synchronization in terms of coefficient C . The map is plotted for three distinct values of external coupling rate $\kappa_e = (0.7\kappa, 0.8\kappa, 0.9\kappa)$, each evaluated at four different values of power $P = (0.9, 1.1, 1.3, 1.5)$. For every values of P 's in the Fig. 6, the region of chaos synchronization with high correlation decreases when κ_e is reduced. This occurs due to the reduced strength of optical field amplitude in the fiber, which are again unable to couple

into the slave due to low coupling rate. However high quality chaos synchronization still persists at lower κ_e at higher P (for example, follow the plots corresponding to $\kappa_e = 0.7\kappa$) since higher P compensate the reduced external coupling strength. On the other hand, the extent of stable complete synchronization line in the plots, corresponding to, for say $\kappa_e = 0.9\kappa$, is more for $P = 0.9$ and $P = 1.1$, which is simply because of the accessibility of wider chaotic regions in those power levels. The numerical study suggest that minimum operable power for complete synchronization is roughly around $P = 0.8$. Now, if we keep on increasing P and goes beyond $P \approx 2.1$, the availability of desired chaotic regions in the master cavity diminishes.

Throughout we assumed $\kappa_{e1} = \kappa_{e2}$, but there may be mismatches in them. In that case, the product $\sqrt{\kappa_{e1} \kappa_{e2}}$ should be maintained at certain critical value to induce complete synchronization, and this information can be extracted from the results in Fig. 6. The necessary magnitude of $\kappa_{e1,2}$, for synchronization, is high and the total cavity decay rate is dominated by this term. Correspond-

ingly, the cavity should be designed with low intrinsic losses (equivalently high quality factor), that is possible with current fabrication methods. Also, the coupling rate $\kappa_{s_{1,2}}$ for the driving laser needs to significantly lower,

which requires high driving laser amplitude $s_{1,2}^{\text{in}}$, implying higher input power. Therefore, increasing $\kappa_{e_{1,2}}$ will impose a lot of practical constraints.

-
- [1] S. H. Strogatz, *Nonlinear dynamics and chaos: with applications to physics, biology, chemistry, and engineering* (CRC press, 2018).
- [2] M. Thiel, J. Kurths, M. C. Romano, G. Károlyi, and A. Moura, *Nonlinear Dynamics and Chaos: Advances and Perspectives* (Springer Berlin, Heidelberg, 2010).
- [3] E. Ott, Strange attractors and chaotic motions of dynamical systems, *Reviews of Modern Physics* **53**, 655 (1981).
- [4] L. M. Pecora and T. L. Carroll, Synchronization in chaotic systems, *Phys. Rev. Lett.* **64**, 821 (1990).
- [5] B. Jovic and B. Jovic, Chaotic signals and their use in secure communications, *Synchronization Techniques for Chaotic Communication Systems*, 31 (2011).
- [6] I. Mishkovski and L. Kocarev, Chaos-based public-key cryptography, in *Chaos-Based Cryptography: Theory, Algorithms and Applications* (Springer, 2011) pp. 27–65.
- [7] M. Zhang, J. Zhang, L. Qiao, and T. Wang, Chaos Brillouin distributed optical fiber sensing, in *Novel Optical Fiber Sensing Technology and Systems* (Springer, 2024) pp. 147–217.
- [8] K. Aihara, T. Takabe, and M. Toyoda, Chaotic neural networks, *Physics letters A* **144**, 333 (1990).
- [9] M. C. Soriano, J. García-Ojalvo, C. R. Mirasso, and I. Fischer, Complex photonics: Dynamics and applications of delay-coupled semiconductor lasers, *Reviews of Modern Physics* **85**, 421 (2013).
- [10] A. Argyris, E. Grivas, M. Hamacher, A. Bogris, and D. Syvridis, Chaos-on-a-chip secures data transmission in optical fiber links, *Optics express* **18**, 5188 (2010).
- [11] G. D. Vanwiggeren and R. Roy, Communication with chaotic lasers, *Science* **279**, 1198 (1998).
- [12] I. Fischer, Y. Liu, and P. Davis, Synchronization of chaotic semiconductor laser dynamics on subnanosecond time scales and its potential for chaos communication, *Physical Review A* **62**, 011801 (2000).
- [13] A. Uchida, T. Heil, Y. Liu, P. Davis, and T. Aida, High-frequency broad-band signal generation using a semiconductor laser with a chaotic optical injection, *IEEE journal of quantum electronics* **39**, 1462 (2003).
- [14] Z. Yang, L. Yi, J. Ke, Q. Zhuge, Y. Yang, and W. Hu, Chaotic optical communication over 1000 km transmission by coherent detection, *Journal of Lightwave Technology* **38**, 4648 (2020).
- [15] N. Jiang, A. Zhao, C. Xue, J. Tang, and K. Qiu, Physical secure optical communication based on private chaotic spectral phase encryption/decryption, *Optics letters* **44**, 1536 (2019).
- [16] O. Junji, *Semiconductor Lasers: Stability, Instability and Chaos* (Springer Cham, 2017).
- [17] M. Aspelmeyer, T. J. Kippenberg, and F. Marquardt, Cavity optomechanics, *Reviews of Modern Physics* **86**, 1391 (2014).
- [18] T. Carmon, M. Cross, and K. J. Vahala, Chaotic quivering of micron-scaled on-chip resonators excited by centrifugal optical pressure, *Physical review letters* **98**, 167203 (2007).
- [19] L. Bakemeier, A. Alvermann, and H. Fehske, Route to chaos in optomechanics, *Physical review letters* **114**, 013601 (2015).
- [20] D. Navarro-Urrios, N. E. Capuj, M. F. Colombano, P. D. García, M. Sledzinska, F. Alzina, A. Griol, A. Martínez, and C. M. Sotomayor-Torres, Nonlinear dynamics and chaos in an optomechanical beam, *Nature communications* **8**, 14965 (2017).
- [21] S. Mondal, M. S. Baptista, and K. Debnath, Chaotic dynamics under the influence of a synthetic magnetic field in an optomechanical system, *Physical Review A* **110**, 023509 (2024).
- [22] D.-W. Zhang, C. You, and X.-Y. Lü, Intermittent chaos in cavity optomechanics, *Physical Review A* **101**, 053851 (2020).
- [23] X.-Y. Lü, H. Jing, J.-Y. Ma, and Y. Wu, Pt-symmetry-breaking chaos in optomechanics, *Physical review letters* **114**, 253601 (2015).
- [24] J. Ma, C. You, L.-G. Si, H. Xiong, J. Li, X. Yang, and Y. Wu, Formation and manipulation of optomechanical chaos via a bichromatic driving, *Physical Review A* **90**, 043839 (2014).
- [25] N. Yang, A. Miranowicz, Y.-C. Liu, K. Xia, and F. Nori, Chaotic synchronization of two optical cavity modes in optomechanical systems, *Scientific Reports* **9**, 15874 (2019).
- [26] F. Monifi, J. Zhang, Ş. K. Özdemir, B. Peng, Y.-x. Liu, F. Bo, F. Nori, and L. Yang, Optomechanically induced stochastic resonance and chaos transfer between optical fields, *Nature Photonics* **10**, 399 (2016).
- [27] A. Pikovsky, M. Rosenblum, and J. Kurths, *Synchronization*, Cambridge university press **12** (2001).
- [28] S. Boccaletti, J. Kurths, G. Osipov, D. Valladares, and C. Zhou, The synchronization of chaotic systems, *Physics reports* **366**, 1 (2002).
- [29] J. S. W. L. Deniz Eroglu and T. Pereira, Synchronisation of chaos and its applications, *Contemporary Physics* **58**, 207 (2017).
- [30] A. Locquet, C. Masoller, and C. R. Mirasso, Synchronization regimes of optical-feedback-induced chaos in unidirectionally coupled semiconductor lasers, *Physical Review E* **65**, 056205 (2002).
- [31] A. Murakami, Synchronization of chaos due to linear response in optically driven semiconductor lasers, *Physical Review E* **65**, 056617 (2002).
- [32] H. J. Eichler, J. Eichler, O. Lux, H. J. Eichler, J. Eichler, and O. Lux, Semiconductor lasers, *Lasers: Basics, Advances and Applications*, 165 (2018).
- [33] S. Acharyya and R. Amritkar, Synchronization of coupled nonidentical dynamical systems, *Europhysics Letters* **99**, 40005 (2012).
- [34] N. F. Rulkov, M. M. Sushchik, L. S. Tsimring, and H. D. Abarbanel, Generalized synchronization of chaos in directionally coupled chaotic systems, *Physical Review E*

- 51, 980 (1995).
- [35] T. Dahms, J. Lehnert, and E. Schöll, Cluster and group synchronization in delay-coupled networks, *Physical Review E—Statistical, Nonlinear, and Soft Matter Physics* **86**, 016202 (2012).
- [36] I. Belykh, V. Belykh, K. Nevidin, and M. Hasler, Persistent clusters in lattices of coupled nonidentical chaotic systems, *Chaos: An Interdisciplinary Journal of Nonlinear Science* **13**, 165 (2003).
- [37] L. M. Pecora, F. Sorrentino, A. M. Hagerstrom, T. E. Murphy, and R. Roy, Cluster synchronization and isolated desynchronization in complex networks with symmetries, *Nature communications* **5**, 4079 (2014).
- [38] C. Zhou and J. Kurths, Noise-induced phase synchronization and synchronization transitions in chaotic oscillators, *Physical review letters* **88**, 230602 (2002).
- [39] I. Z. Kiss and J. L. Hudson, Phase synchronization of nonidentical chaotic electrochemical oscillators, *Physical Chemistry Chemical Physics* **4**, 2638 (2002).
- [40] Y. Sugitani, Y. Zhang, and A. E. Motter, Synchronizing chaos with imperfections, *Physical review letters* **126**, 164101 (2021).
- [41] T. Kippenberg, H. Rokhsari, T. Carmon, A. Scherer, and K. Vahala, Analysis of radiation-pressure induced mechanical oscillation of an optical microcavity, *Physical Review Letters* **95**, 033901 (2005).
- [42] A. Schliesser, G. Anetsberger, R. Rivière, O. Arcizet, and T. J. Kippenberg, High-sensitivity monitoring of micromechanical vibration using optical whispering gallery mode resonators, *New Journal of Physics* **10**, 095015 (2008).
- [43] S. Weis, R. Rivière, S. Deléglise, E. Gavartin, O. Arcizet, A. Schliesser, and T. J. Kippenberg, Optomechanically induced transparency, *science* **330**, 1520 (2010).
- [44] C. Caucheteur, A. Mussot, S. Bette, A. Kudlinski, M. Douay, E. Louvergneaux, P. Mégret, M. Taki, and M. González-Herráez, All-fiber tunable optical delay line, *Optics Express* **18**, 3093 (2010).
- [45] X. Wang, L. Zhou, R. Li, J. Xie, L. Lu, K. Wu, and J. Chen, Continuously tunable ultra-thin silicon waveguide optical delay line, *Optica* **4**, 507 (2017).
- [46] C. Manolatou, M. Khan, S. Fan, P. Villeneuve, H. Haus, and J. Joannopoulos, Coupling of modes analysis of resonant channel add-drop filters, *IEEE Journal of Quantum Electronics* **35**, 1322 (1999).
- [47] T. F. Roque, F. Marquardt, and O. M. Yevtushenko, Nonlinear dynamics of weakly dissipative optomechanical systems, *New Journal of Physics* **22**, 013049 (2020).
- [48] L. Koehler, P. Chevalier, E. Shim, B. Desiatov, A. Shams-Ansari, M. Piccardo, Y. Okawachi, M. Yu, M. Loncar, M. Lipson, *et al.*, Direct thermo-optical tuning of silicon microresonators for the mid-infrared, *Optics express* **26**, 34965 (2018).
- [49] K. N. Dinyari, R. J. Barbour, D. A. Golter, and H. Wang, Mechanical tuning of whispering gallery modes over a 0.5 thz tuning range with mhz resolution in a silica microsphere at cryogenic temperatures, *Optics Express* **19**, 17966 (2011).
- [50] C. Bekker, C. G. Baker, R. Kalra, H.-H. Cheng, B.-B. Li, V. Prakash, and W. P. Bowen, Free spectral range electrical tuning of a high quality on-chip microcavity, *Optics express* **26**, 33649 (2018).
- [51] D. J. Gauthier and J. C. Bienfang, Intermittent loss of synchronization in coupled chaotic oscillators: Toward a new criterion for high-quality synchronization, *Physical Review Letters* **77**, 1751 (1996).
- [52] J. Lu, G. Yang, H. Oh, and A. C. Luo, Computing lyapunov exponents of continuous dynamical systems: method of lyapunov vectors, *Chaos, Solitons & Fractals* **23**, 1879 (2005).
- [53] H. Dedieu, M. P. Kennedy, and M. Hasler, Chaos shift keying: modulation and demodulation of a chaotic carrier using self-synchronizing chua’s circuits, *IEEE Transactions on Circuits and Systems II: Analog and Digital Signal Processing* **40**, 634 (1993).